ORGANIC CHEMISTRY FRONTIERS

RESEARCH ARTICLE

View Article Online
View Journal | View Issue

Cite this: *Org. Chem. Front.*, 2023, **10**, 3485

The role of attractive dispersion interaction in promoting the catalytic activity of asymmetric hydrogenation†

Limin Yang, *[a,b] Bo Li[c] and K. N. Houk *[b]

Received 3rd March 2023,
Accepted 17th June 2023

DOI: 10.1039/d3qo00332a

rsc.li/frontiers-organic

As an essential van der Waals interaction, the dispersion interaction is an important weak attractive interaction. However, the influence of the weak attractive interactions has only recently been elucidated in transition metal catalyzed asymmetric hydrogenations by the Wanbin Zhang group. Our IGM/EDA analysis proves Zhang's finding that attractive interactions play an important role in asymmetric hydrogenation, which provides new strategies for the sophisticated design of chiral transition metal catalysts. The dispersion interaction is the major weak attractive interaction that activates the asymmetric hydrogenations by favorable interactions of substrate and metal catalyst.

Introduction

Attractive dispersion interactions, a van der Waals interaction also called London dispersion interactions, have only recently been studied in organic reactions because of the development of practical computational methods to compute such interactions.[1] Recently, dispersion interactions have been recognized to play an important role in influencing reactivity and stereoselectivity in enzyme- and organo-catalyzed asymmetric reactions.[1–4] However, the significant effects of attractive dispersion interactions between substrate and ligand have been described only in a few homogeneous transition-metal catalyzed asymmetric transformations.[5,6]

Transition-metal catalyzed asymmetric hydrogenation of unsaturated substrates is one of the most important transformations for preparing chiral products. Over the past half century, numerous catalysts based on chiral ligands coordinated with noble–metals have been designed, synthesized, and evaluated for catalytic selectivity and efficiency, and a series of highly efficient asymmetric hydrogenation reactions have been developed.[7] Although some noble–metals, such as Rh, Ru, and Ir, catalyzed asymmetric hydrogenations have been applied in industry, their high cost and toxicity have prevented them from broad application.[8]

In order to control the cost and reduce the toxicity of chiral catalysts in asymmetric hydrogenations, earth-abundant transition metal catalysts have been considered as alternatives due to their abundance, low cost, and environmental friendliness. However, compared with asymmetric hydrogenation catalyzed by noble–metals, their catalytic efficiency is generally very low, and they have not been used in industry.[9]

To tackle the challenges mentioned above, Wanbin Zhang group at Shanghai Jiao Tong University has improved significantly the catalytic efficiency of the earth-abundant transition metal nickel catalyzed asymmetric hydrogenations by exploiting attractive weak interactions between the ligand and substrate existing in the key transition state structure. This group published a series of papers in *Angew. Chem.*, *Nat. Commun.* and *Nat. Chem.*, describing their discoveries.[10–16] In these studies, weak attractive interactions have been found to play an important role by stabilizing the favorable key transition state structure formed by chiral catalysts and substrates and promoting the hydrogenation reaction. These weak attractive interactions could be found as CH···HC, CH···π, CH···O, and other interactions in Zhang and his coworkers' work. However, after summarizing these works, we believe there is a key interaction dominating the weak interaction, therefore, a series of analysis has been proceeded and proved the dispersion interaction as the major weak interaction.

Results and discussion

At first, IGM[17,18] (Independent Gradient Model) analysis has been carried out to identify the location of the interactions based on the Wanbin Zhang group's original DFT compu-

[a]*College of Material, Chemistry and Chemical Engineering, Hangzhou Normal University, Hangzhou, Zhejiang 311121, China. E-mail: myang@hznu.edu.cn*
[b]*Department of Chemistry and Biochemistry, University of California, Los Angeles, CA 90095-1569, USA. E-mail: houk@chem.ucla.edu*
[c]*Division of Chemistry and Chemical Engineering, California Institute of Technology, Pasadena, CA 91125, USA*

† Electronic supplementary information (ESI) available. See DOI: https://doi.org/10.1039/d3qo00332a

tational structures. It should be noted that IGM methods are inspired by the RDG approach (also known as NCI analysis),[19] and intermolecular interactions do not interfere with intramolecular interactions in IGM unlike RDG analyses.[17] The figure notes and graphic symbols of IGM analysis are listed in Fig. 1.

Second, we performed EDA (Energy Decomposition Analysis) to identify the specific weak interaction quantitatively.[20] This EDA is aimed at the interaction between substrate and metal complex. The total interaction energy, marked as E_{total}, has been divided into six parts: the electrostatic interaction (E_{ele}), the exchange repulsion interaction (E_{ex}), the induction interaction (E_{ind}), the dispersion interaction (E_{disp}), the distortion of substrate ($E_{dist(sub)}$), and the distortion of metal complex ($E_{dist(cat)}$). In general, the total interaction energies E_{total} are always negative and the relative level of energies are corresponded to the free energies in the manuscript. E_{ele} (always positive) represents the coordination interaction in these computations, E_{ind} (always negative) represents interaction between dipole and induced dipole like C–H···O or C–H···π, and E_{disp} (always negative) represents interaction between instantaneous dipoles like C–H···H–C. $E_{dist(sub)}$ and $E_{dist(cat)}$ represent distortion of substrate and the distortion of metal complex respectively, which are always positive. According to these studies, dispersion interactions (CH···HC interactions) have the potential to enhance the reactivity of hydrogenations, resulting in a high S/C (Substrate/Catalyst, mole ratio) value and in some cases the stereoselectivity.

Compared with the noble–metal Rh, Ru, and Ir catalysts, only a few efficient Pd-catalyzed asymmetric hydrogenations have been reported. In 2018, W. Zhang and coworkers initially reported a highly efficient $Pd(OAc)_2$-catalyzed asymmetric hydrogenation of sterically hindered *N*-sulfonyl imines (Fig. 2A).[10] By employing a cheap palladium salt $Pd(OAc)_2$ with low toxicity and (*R*,*R*)-QuinoxP* as ligand, highly catalytic activity and enantioselectivity were observed (up to 99% yield, 99% ee, and 5000 S/C) in the reaction. In the ligand screening of the reaction, normal aryl-substituted diphosphine ligand with axial chirality like (*R*)-BINAP gave no desired product. Only by using alkyl-substituted phosphine ligands, the reaction would occur. And the yield increased as the increase of the substituents of the alkyl groups.

In Zhang's report, computational investigation and control experiments revealed that the high catalytic efficiency originates from the significant structural differences caused by

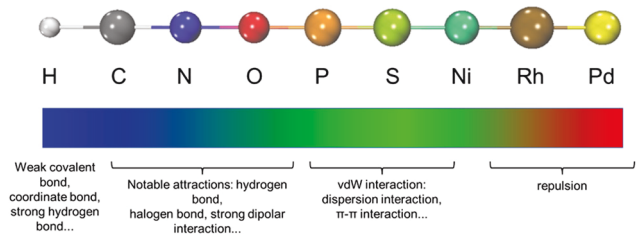

Fig. 1 Figure notes and graphic symbols of IGM analysis.

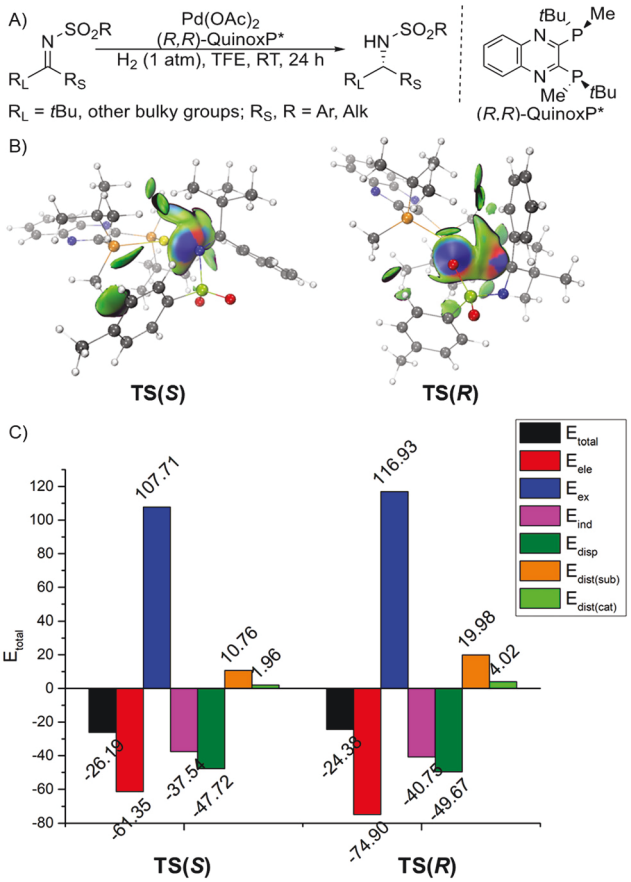

Fig. 2 (A) Hydrogenation of *N*-sulfonyl imines; (B) IGM analysis of **TS(*S*)** and **TS(*R*)**; (C) EDA analysis of **TS(*S*)** and **TS(*R*)**.

weak attractive interactions between the catalyst and substrate. Our IGM and EDA analysis further shows the existing of strong and significant attractive dispersion interactions (Fig. 2B), with the large E_{disp} (compared with E_{ind}) in the EDA (Fig. 2C). The dispersion interactions could be found both in **TS(*R*)** and in **TS(*S*)**, thus increase the reactivity efficiently. Even though **TS(*S*)** with the lower activation energy in Fig. 2 has a relatively weaker attractive dispersion interaction (E_{disp} = −47.72 kcal mol^{-1}) than that of **TS(*R*)** (E_{disp} = −49.67 kcal mol^{-1}), without these dispersion interactions, the reaction does not occur smoothly. These IGM/EDA analyses indicated the dominance of dispersion interactions, and was consistent with the experimental data mentioned above.

Chiral α-amino aldehydes have a wide range of potential applications in organic synthesis and medicinal chemistry. To synthesize chiral α-amino aldehydes with high efficiency, W. Zhang and coworkers reported a highly efficient Rh-catalyzed asymmetric hydrogenation of α-formyl enamides using BenzP* as ligand, affording chiral α-amino aldehydes with up to 20 000 S/C.[11] Again, normal aryl-substituted diphosphine ligand with axial chirality like (*R*)-BINAP gave no desired product. Yet the reaction occurs with alkyl-substituted phosphine ligands. Zhang's DFT computational investigation revealed that the weak interactions between the ligand and

substrate are the crucial features in the formation of key intermediates (Fig. 3A). The IGM shows the interactions between substrates and metal catalyst (Fig. 3B). However, our further EDA analysis shows a different view of weak interactions (Fig. 3C). In intermediate **25**, the E_{ind} dominates the weak interactions. However, this intermediate is too stable and hardly reacts, only leading to unfavored product. For the actual reacted intermediate **18**, dispersion interactions promote the hydrogenation. These analyses indicated the dominance of dispersion interactions, and are consistent with the experimental data mentioned above.

Zhang's coworkers, Chen and D. Gridnev studied the weak interactions in catalytic hydrogenation with DFT in 2020.[21] They studied the asymmetric hydrogenation of α-acyloxy-1-arylethanones *via* Pd and (*R*)-DTBM-Segphos, studied by Zhang and coworkers in 2013 (Fig. 4A).[22] This example compared the energy barrier of hydrogenation with (*R*)-DTBM-Segphos and (*R*)-Segphos. With (*R*)-DTBM-Segphos which is considered to have large steric hindrance, the energy barrier was about 7.6 kcal mol^{-1} lower than with (*R*)-Segphos, that does not have the two bulky *tert*-butyl groups. The result matched the experimental yield of standard substrate >99% (with (*R*)-DTBM-Segphos) and <5% (with (*R*)-Segphos) respectively.

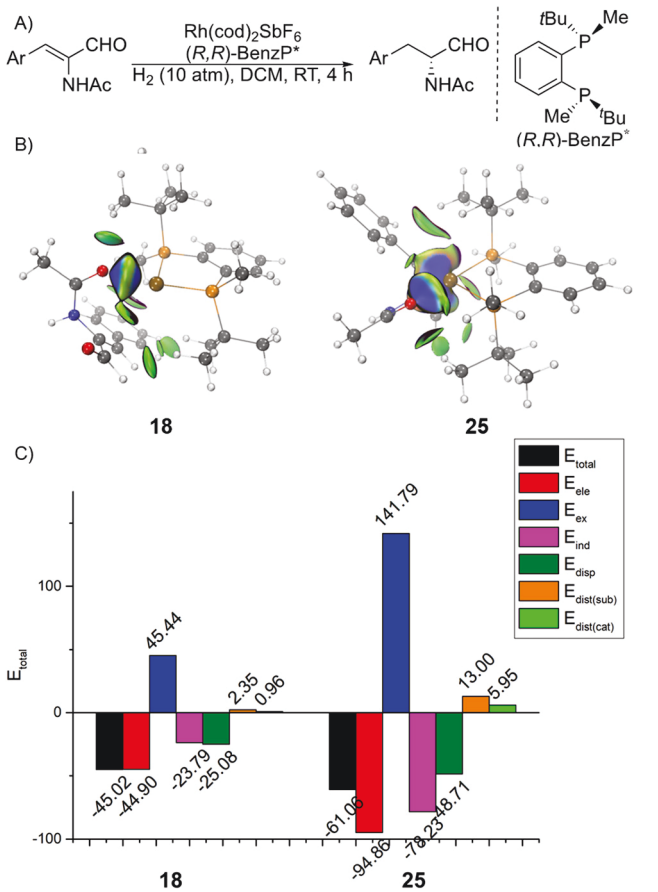

Fig. 3 (A) Hydrogenation in α-formyl enamides; (B) IGM analysis of **18** and **25**; (C) EDA analysis of **18** and **25**.

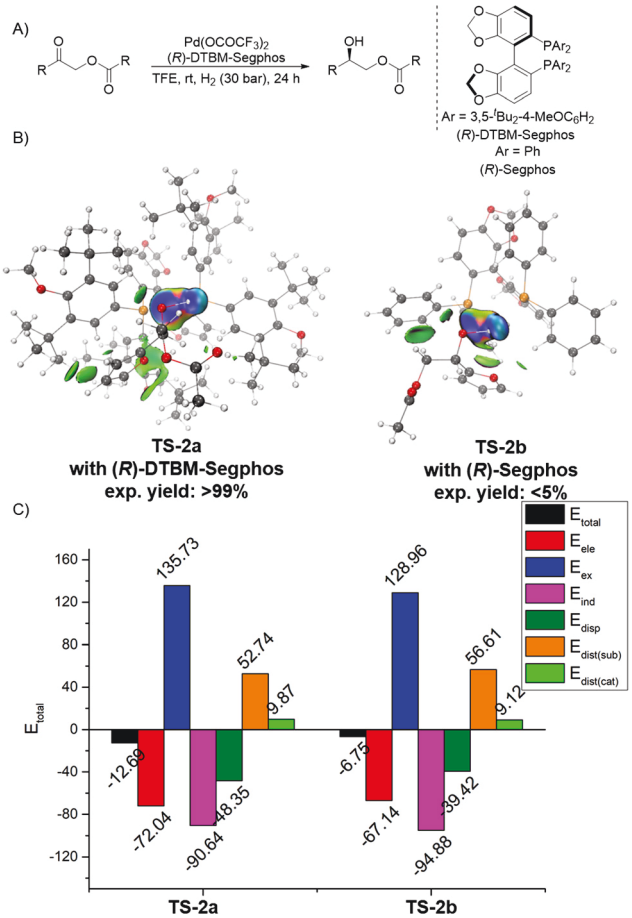

Fig. 4 (A) Hydrogenation in α-acyloxy-1-arylethanones; (B) IGM analysis of **TS-2a** and **TS-2b**; (C) EDA analysis of **TS-2a** and **TS-2b**.

According to the IGM analysis, there are more attractive dispersion interactions in **TS-2a**, especially near the *tert*-butyl groups of (*R*)-DTBM-Segphos. In **TS-2b**, fewer attractive dispersion interactions are found (Fig. 4B). The enantioselective step is the heterolysis of H_2, and the EDA shows large induction interaction energies and high distortion energies of substrate. However, these do not affect the analysis of attractive dispersion interactions. With *tert*-butyl groups the E_{disp} of **TS-2a** is −48.4 kcal mol^{-1}, much larger than the E_{disp} of **TS-2b** −39.5 kcal mol^{-1} (Fig. 4C). Dispersion also contributes most to the decrease of the activation energy (see ESI, Table S3†).

Based on the above mentioned Pd- and Rh-catalyzed asymmetric hydrogenations utilizing weak attractive interactions, Zhang's group turned to the first-row earth-abundant transition metal nickel catalyzed asymmetric hydrogenations. They reported an efficient earth-abundant metal nickel catalyzed asymmetric hydrogenation of *N*-sulfonyl imines almost at the same time as the previous investigations (Fig. 5A). The active (*R*,*R*)-QuinoxP*–Ni complex existing in the equilibrium to excess $Ni(OAc)_2$ improved the hydrogenation efficiency and provided chiral *t*-Bu-sulfonyl amines with high yields and excellent enantioselectivities (up to 99% yield and 99% ee).[12] A

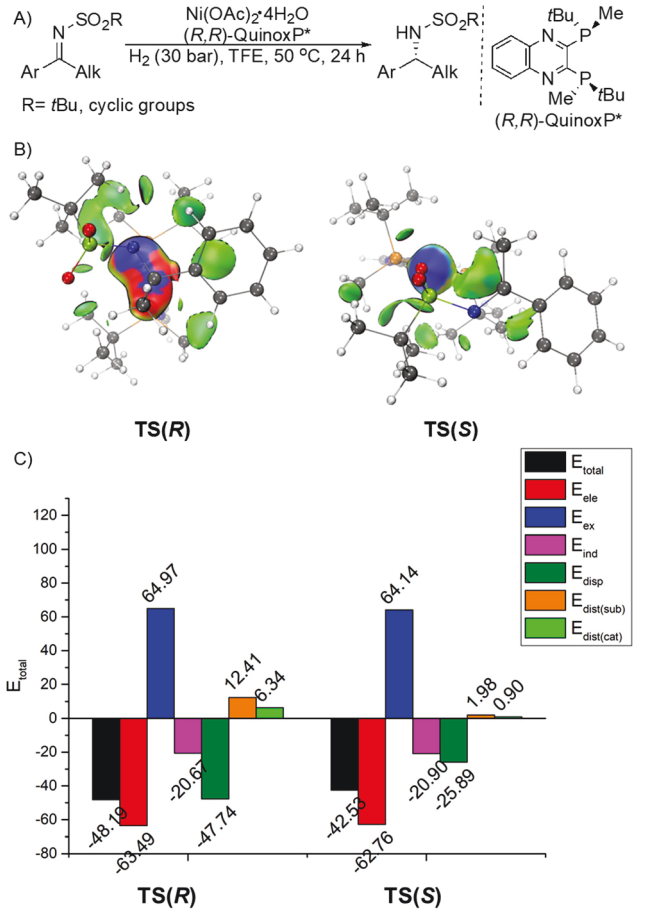

Fig. 5 (A) Hydrogenation of *N*-sulfonyl imines; (B) IGM analysis of **TS(*R*)** and **TS(*S*)**; (C) EDA analysis of **TS(*R*)** and **TS(*S*)**.

dramatically decreased catalyst loading (10 500 S/C) represents the best catalytic behavior for the reported nickel-catalyzed asymmetric hydrogenations. Similarly, normal aryl-substituted diphosphine ligand with axial chirality like (*S*)-BINAP or (*S*)-Segphos gave desired product with low yield (51% and 38%, respectively). By introducing *tert*-butyl group in the P atom of the phosphine ligand, the reaction proceeded smoothly. Larger version of (*S*)-Segphos, (*S*)-DTBM-Segphos can also promote the reaction, though the selectivity was not satisfactory (58%). Nevertheless, these results indicate the importance of dispersion interactions. According to Zhang's DFT computational investigation, dispersion interactions play an essential role in the high catalytic efficiency and excellent enantioselectivity origination. The quantitative difference of CH···HC interactions was found between the *R*- and *S*-transition state structures, partly accounting for the results, and revealing the effect of the *tert*-butyl group. The IGM analysis shows multiple dispersion interactions around the *tert*-butyl group, revealing its importance in the combination of the catalyst with substrates (Fig. 5B).

Also, our further EDA shows that the dispersion interaction is the major weak interaction in **TS(*R*)**, significantly stronger than that in **TS(*S*)** (−47.74 kcal mol^{-1} *vs.* −25.89 kcal mol^{-1}, Fig. 5C). According to the IGM analysis of **TS(*R*)**, the *tert*-butyl of substrate shows obvious interaction with the *tert*-butyl in the ligand, while lesser interactions are found in **TS(*S*)** (Fig. 5B), consistent with Zhang's results as well. In this example, dispersion interaction not only improved the reactivity but also the enantioselectivity of the asymmetric hydrogenation reaction. On this basis, W. Zhang also developed the efficient Ni-catalyzed asymmetric hydrogenations for the synthesis of α-phenylalanines and α-phenylglycines.[13,14] In these cases, only when using alkyl-substituted phosphine, especially *tert*-butyl substituted ligands, the reaction could occur successfully.

In 2022, the W. Zhang group reported the development of an environmentally friendly, earth-abundant, transition-metal nickel catalyzed asymmetric hydrogenation of oximes, remaining challenge due to the labile N–O bond and sluggish C=N bond (Fig. 6A).[15] By employing a readily available (*S*,*S*)-Ph–BPE–Ni complex catalyst, the hydrogenation of oximes proceeded smoothly to enantiomerically enriched hydroxylamines with up to 99% yield, 99% ee and with 1000 S/C. Normal aryl-substituted diphosphine ligand with axial chirality like (*S*)-BINAP or (*S*)-Segphos gave desired product with low yield as

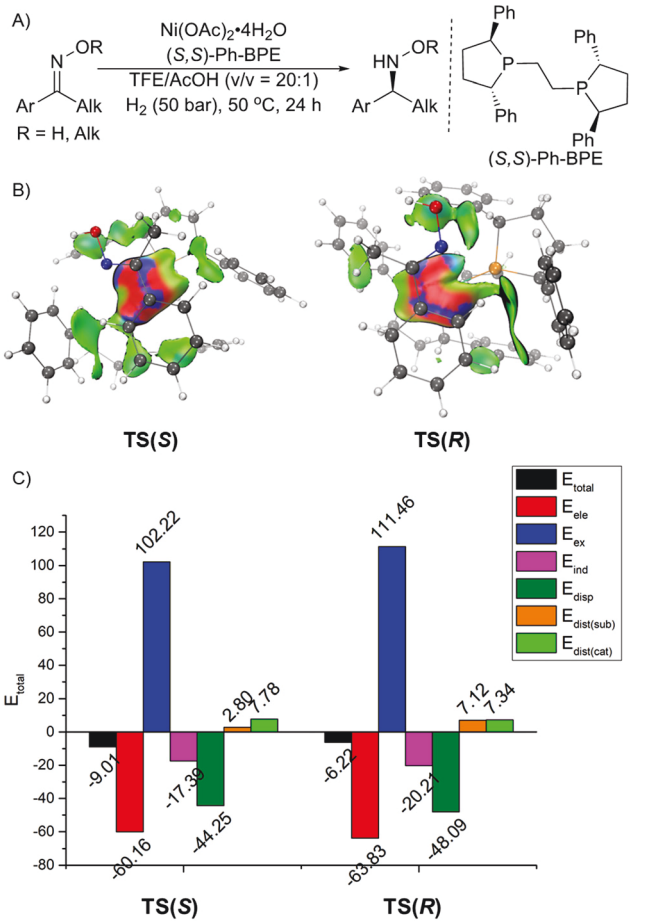

Fig. 6 (A) Hydrogenation of oximes; (B) IGM analysis of **TS(*S*)** and **TS(*R*)**; (C) EDA analysis of **TS(*S*)** and **TS(*R*)**.

well (7% and 50%, respectively). The ligand with phospholane skeleton like (*S*,*S*)-Ph–BPE behaved well. DFT computation results indicated that the hydrogenation efficiency and enantioselectivity were facilitated by multiple weak interactions between the Ni-catalyst and oxime substrate. In Zhang's work, weak attractive interactions were found in the structures of **TS(*R*)** and **TS(*S*)**, playing crucial roles by lowering the reaction barriers, thus raising the reaction efficiency. We found that because only non-polar groups exist in the ligand, no obvious hydrogen bond with hydroxyl group was observed. Instead, there are a lot of C–H···H–C and C–H···π interactions between substrates and catalysts in the IGM analysis (Fig. 6B).

The EDA shows stronger dispersion interactions than the induction interactions (Fig. 6C), exhibiting the importance of dispersion interactions between substrates and metal catalysts. Though **TS(*S*)** with the lower activation energy in Fig. 6 has a relatively weaker attractive dispersion interaction (E_{disp} = −44.3 kcal mol^{-1}) than that of **TS(*R*)** (E_{disp} = −48.1 kcal mol^{-1}), without these dispersion interactions provided from the special phospholane skeleton, the reaction did not occur smoothly.

Very recently, the W. Zhang group reported another efficient nickel catalyzed asymmetric hydrogenation of α-substituted vinylphosphonates and diarylvinylphosphine oxides, affording corresponding chiral α-substituted ethylphosphonate and ethylphosphine oxide compounds with 99% yield, 96% ee and 1000 S/C, which are widely used in drugs, pesticides, and ligands (Fig. 7A).[16] The hydrogenation reactivity was high even with aryl-substituted ligands. However, the enantioselectivity of the reaction showed it was sensitive to the alkyl group of the phosphate (R group in Fig. 7A). The ee increased from 88% to 91% when switching the R group from OEt to O^{i}Pr, indicating that dispersion interactions increase the enantioselectivity. Zhang's DFT calculation shows that the weak attractive interactions between the catalyst and the terminal olefin substrate in **TS(*R*)** are greater than those in **TS(*S*)**, which play important roles in the transition states and could lower the barrier of reduction for the olefins.

According to our IGM analysis, interactions between the *tert*-butyl group on the ligand and benzyl group of the substrate and the interactions between the *tert*-butyl group on the ligand and isopropyl group of the substrate guarantee the lower energy of **TS(*R*)**, benefiting from the *tert*-butyl group of the ligand (Fig. 7B). This reflects the stronger dispersion energies compared with induction energies in EDA (Fig. 7C), thus increase the reactivity. Though **TS(*R*)** with the lower activation energy in Fig. 7 has a relatively weaker attractive dispersion interaction (E_{disp} = −32.1 kcal mol^{-1}) than that of **TS(*S*)** (E_{disp} = −38.4 kcal mol^{-1}), the additional Ni–O bond provided extra stabilization energy (E_{ele}). However, this additional bond is not affected by the R group of the phosphate. Even if there was influence, the larger steric hindrance of the R group (O^{i}Pr) should weaken this bond, yet the O^{i}Pr increase the ee value. Without the larger alkyl group, the difference of E_{disp} between two transition states could be larger; the dispersion interaction increased enantioselectivity in this case. On the other hand,

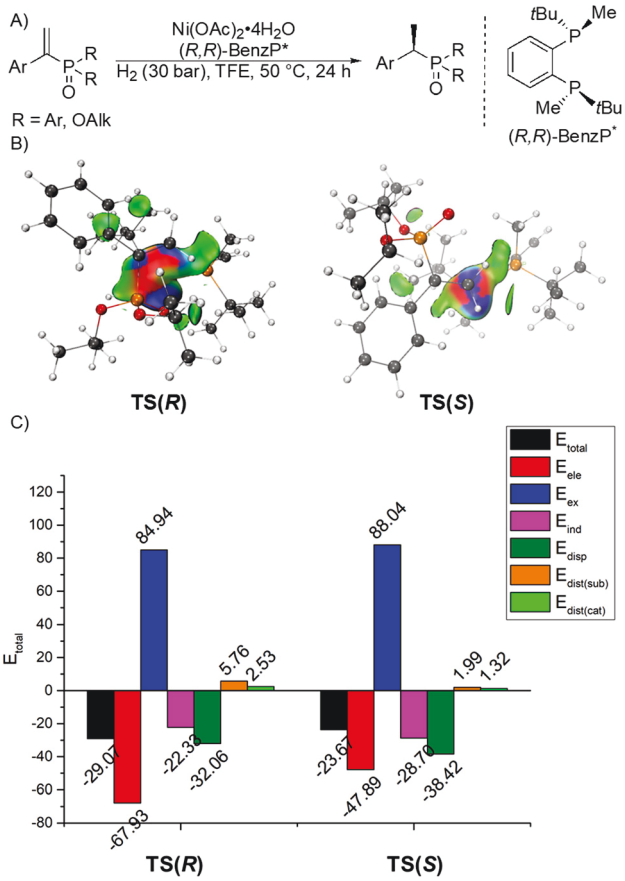

Fig. 7 (A) Hydrogenation of diisopropyl (1-phenylvinyl)phosphonate; (B) IGM analysis of **TS(*R*)** and **TS(*S*)**; (C) EDA analysis of **TS(*R*)** and **TS(*S*)**.

when using aryl-substituted ligands with the same C_2 symmetry, the reaction gave desired products with low enantioselectivity (63%–82% ee), indicating that the dispersion interactions promoted the enantioselectivity. Both Zhang's DFT computational result and our IGM/EDA analysis indicated the dominance of dispersion interactions, and are consistent with the experimental data mentioned above.

Conclusions

Our IGM/EDA analysis further demonstrates that the Zhang group has discovered an important role of weak attractive interactions in asymmetric catalytic hydrogenations, which provides a new strategy for the sophisticated design of chiral transition metal catalysts involving both noble and earth-abundant metals. In addition, we show that the dispersion interactions activate the asymmetric hydrogenation reaction by the favorable interaction between substrate and metal catalyst. Based on these interactions, W. Zhang and coworkers developed several highly efficient asymmetric hydrogenations of *N*-sulfonyl imines, α-formyl enamides, oximes and α-substituted vinylphosphonates using chiral transition-metal catalysts derived from noble to earth-abundant metals, produ-

cing the corresponding chiral compounds with high yields, enantioselectivities, and S/C ratios.

Conflicts of interest

The authors declare no conflict of interest.

Acknowledgements

We gratefully acknowledge the National Science Foundation (CHE-1764328 to K. N. H.), the National Natural Science Foundation of China (Grant 22271071 to L. Y.), and the Natural Science Foundation of Zhejiang Province (Grant LY20B020010 to L. Y.) for financial support.

References

1 J. P. Wagner and P. R. Schreiner, London Dispersion in Molecular Chemistry-Reconsidering Steric Effects, *Angew. Chem., Int. Ed.*, 2015, **54**, 12274–12296.
2 M. Bursch, E. Caldeweyher, A. Hansen, H. Neugebauer, S. Ehlert and S. Grimme, Understanding and Quantifying London Dispersion Effects in Organometallic Complexes, *Acc. Chem. Res.*, 2019, **52**, 258–266.
3 P. H.-Y. Cheong, C. Y. Legault, J. M. Um, N. Çelebi-Ölçüm and K. N. Houk, Quantum Mechanical Investigations of Organocatalysis: Mechanisms, Reactivities, and Selectivities, *Chem. Rev.*, 2011, **111**, 5042–5137.
4 S. E. Wheeler, T. J. Seguin, Y. Guan and A. C. Doney, Noncovalent Interactions in Organocatalysis and the Prospect of Computational Catalyst Design, *Acc. Chem. Res.*, 2016, **49**, 1061–1069.
5 G. Lu, R. Y. Liu, Y. Yang, C. Fang, D. S. Lambrecht, S. L. Buchwald and P. Liu, Ligand–Substrate Dispersion Facilitates the Copper-Catalyzed Hydroamination of Unactivated Olefins, *J. Am. Chem. Soc.*, 2017, **139**, 16548–16555.
6 B. Li, H. Xu, Y. Dang and K. N. Houk, Dispersion and Steric Effects on Enantio-/Diastereoselectivities in Synergistic Dual Transition-Metal Catalysis, *J. Am. Chem. Soc.*, 2022, **144**, 1971–1985.
7 H. Wang, J. Wen and X. Zhang, Chiral Tridentate Ligands in Transition Metal-Catalyzed Asymmetric Hydrogenation, *Chem. Rev.*, 2021, **121**, 7530–7567.
8 K. Püntener and M. Scalone, in *Enantioselective Hydrogenation: Applications in Process R&D of Pharmaceuticals*, ed. H. U. Blaser and H. J. Federsel, Wiley-VCH, Weinheim, Germany, 2010, ch. 2.
9 J. Wen, F. Wang and X. Zhang, Asymmetric Hydrogenation Catalyzed by First-row Transition Metal Complexes, *Chem. Soc. Rev.*, 2021, **50**, 3211–3237.
10 J. Chen, Z. Zhang, B. Li, F. Li, Y. Wang, M. Zhao, I. D. Gridnev, T. Imamoto and W. Zhang, $Pd(OAc)_2$-C atalyzed Asymmetric Hydrogenation of Sterically Hindered *N*-tosylimines, *Nat. Commun.*, 2018, **9**, 5000.
11 J. Zhang, J. Jia, X. Zeng, Y. Wang, Z. Zhang, I. D. Gridnev and W. Zhang, Chemo- and Enantioselective Hydrogenation of α-Formyl Enamides: An Efficient Access to Chiral α-Amido Aldehydes, *Angew. Chem., Int. Ed.*, 2019, **58**, 11505–11512.
12 B. Li, J. Chen, Z. Zhang, I. D. Gridnev and W. Zhang, Ni-Catalyzed Asymmetric Hydrogenation of N-Sulfonyl Imines, *Angew. Chem., Int. Ed.*, 2019, **58**, 7329–7334.
13 Y. Hu, J. Chen, B. Li, Z. Zhang, I. D. Gridnev and W. Zhang, Nickel–Catalyzed Asymmetric Hydrogenation of 2-Amidoacrylates, *Angew. Chem., Int. Ed.*, 2020, **59**, 5371–5375.
14 D. Liu, B. Li, J. Chen, I. D. Gridnev, D. Yan and W. Zhang, Ni-Catalyzed Asymmetric Hydrogenation of *N*-Aryl Imino Esters for the Efficient Synthesis of Chiral α-Aryl Glycines, *Nat. Commun.*, 2020, **11**, 5935.
15 B. Li, J. Chen, D. Liu, I. D. Gridnev and W. Zhang, Nickel-Catalysed Asymmetric Hydrogenation of Oximes, *Nat. Chem.*, 2022, **14**, 920–927.
16 H. Wei, H. Chen, J. Chen, I. D. Gridnev and W. Zhang, Nickel-Catalyzed Asymmetric Hydrogenation of α-Substituted Vinylphosphonates and Diarylvinylphosphine Oxides, *Angew. Chem., Int. Ed.*, 2023, **62**, e202214990.
17 C. Lefebvre, G. Rubez, H. Khartabil, J.-C. Boisson, J. Contreras-García and E. Hénon, Accurately Extracting the Signature of Intermolecular Interactions Present in the NCI Plot of the Reduced Density Gradient Versus Electron Density, *Phys. Chem. Chem. Phys.*, 2017, **19**, 17928–17936.
18 For selected papers using IGM analysis: (*a*) W. Liu, C. L. Stern and J. F. Stoddart, Suit[4]ane, *J. Am. Chem. Soc.*, 2020, **142**, 10273–10278; (*b*) S. Gao, M. Duan, L. R. Andreola, P. Yu, S. E. Wheeler, K. N. Houk and M. Chen, Unusual Enantiodivergence in Chiral Brønsted Acid-Catalyzed Asymmetric Allylation with β-Alkenyl Allylic Boronates, *Angew. Chem., Int. Ed.*, 2022, **61**, e202208908; (*c*) W. Zhang, L. Chen, S. Dai, C. Zhao, C. Ma, L. Wei, M. Zhu, S. Y. Chong, H. Yang, L. Liu, Y. Bai, M. Yu, Y. Xu, X.-W. Zhu, Q. Zhu, S. An, R. S. Sprick, M. A. Little, X. Wu, S. Jiang, Y. Wu, Y.-B. Zhang, H. Tian, W.-H. Zhu and A. I. Cooper, Reconstructed Covalent Organic Frameworks, *Nature*, 2022, **604**, 72–79.
19 E. R. Johnson, S. Keinan, P. Mori-Sánchez, J. Contreras-García, A. J. Cohen and W. Yang, Revealing Noncovalent Interactions, *J. Am. Chem. Soc.*, 2010, **132**, 6498–6506.
20 B. Jeziorski, R. Moszynski and K. Szalewicz, Perturbation Theory Approach to Intermolecular Potential Energy Surfaces of van der Waals Complexes, *Chem. Rev.*, 1994, **94**, 1887–1930.
21 J. Chen and I. D. Gridnev, Size is Important: Artificial Catalyst Mimics Behavior of Natural Enzymes, *iScience*, 2020, **23**, 100960.
22 J. Chen, D. Liu, N. Butt, C. Li, D. Fan, Y. Liu and W. Zhang, Palladium-Catalyzed Asymmetric Hydrogenation of α-Acyloxy-1-arylethanones, *Angew. Chem., Int. Ed.*, 2013, **52**, 11632–11636.

